07,13

Barocaloric properties of ceramic $(NH_4)_3H(SO_4)_2$

© V.S. Bondarev[1,2], E.A. Mikhaleva[1], M.V. Gorev[1,2], A.V. Kartashev[1,4], M.S. Molokeev[1,2], E.V. Bogdanov[1,3], A.I. Zaytsev[1], I.N. Flerov[1,¶]

[1] Kirensky Institute of Physics, Federal Research Center KSC SB, Russian Academy of Sciences, Krasnoyarsk, Russia
[2] Siberian Federal University, Institute of Engineering Physics and Radio Electronics, Krasnoyarsk, Russia
[3] Institute of Engineering Systems and Energy, Krasnoyarsk State Agrarian University, Krasnoyarsk, Russia
[4] Krasnoyarsk State Medical University named after Prof. V.F. Voyno-Yasenetsky, Krasnoyarsk, Russia

¶E-mail: flerov@iph.krasn.ru

Received August 2, 2024
Revised September 13, 2024
Accepted September 17, 2024

An experimental study of the heat capacity, thermal expansion, and the effect of hydrostatic pressure on the permittivity of ceramics $(NH_4)_3H(SO_4)_2$ was carried out in the region of low-temperature phase transitions $A2/a \leftrightarrow (P2/n)_1 \leftrightarrow (P2/n)_2 \leftrightarrow P\text{-}1$. The main thermodynamic characteristics were determined: entropy, deformation and baric coefficients associated with successive distortions of the crystal lattice. The position of the boundaries between phases $(P2/n)_1$, $(P2/n)_2$ and $P\text{-}1$ in the temperature — pressure diagram was clarified. Based on the analysis of the $S(T, p)$ functions, the values and character of the temperature and baric behavior of the parameters of extensive and intensive barocaloric effects are determined. The absence of temperature hysteresis and a wide range of anomalous heat capacity during the $A2/a \leftrightarrow P2/n$ transition ensure high reproducibility of thermo- and barocycling processes and significant relative cooling capacity of $(NH_4)_3H(SO_4)_2$.

Keywords: phase transitions, heat capacity, thermal expansion, pressure, barocaloric effect.

DOI: 10.61011/PSS.2024.10.59634.244

1. Introduction

Compounds with monovalent cations and the general formulas $A^+(A')^+(S/Se)O_4$ and $(A^+)_xH[(S/Se)O_4]_y$ ($A^+(A')^+$: Na, K, NH_4, Rb, Cs; $x = 1, 3$; $y = 1, 2$) are distinguished among numerous complex sulfates/selenates by the high susceptibility of the structure to changes of temperature, external and internal (chemical) pressures, which leads to a rich variety of phase transitions, including ferroid nature. Rare mineral letovicite — triammonium hydrodisulfate — $(NH_4)_3H(SO_4)_2$ (TAHS) [1] belongs to that particular kind of compounds, however, it is quite easily synthesized and grown in the form of single crystals in laboratory conditions.

Despite many years of active studies on the structure and physical properties of TAHS, interest in this material remains literally to the present time [2–18]. The main reason for the increased attention is determined by the following circumstances. Firstly, TAHS is ferroelastic at room temperature and atmospheric pressure and it experiences a rich sequence of phase transitions II $(A2/a)$ $T_2 = 265\,\text{K} \leftrightarrow \text{III}\,(P2/n)_1$ $T_3 = 140\,\text{K} \leftrightarrow \text{IV}\,(P2/n)_2$ $T_4 = 133\,\text{K} \leftrightarrow \text{V}\,(P\text{-}1)$ $T_5 = 63\,\text{K} \leftrightarrow \text{VII}\,(P1)$ in case of cooling. Henceforward, the generally accepted numbering of phases and temperatures of phase transformations is used [3,8,16,19]. Secondly, unlike other ammonium hydrosulfates/selenates, the ferroelectric state in TAHS (phase VII $(P1)$) occurs at atmospheric pressure as a result of a phase transition of the first kind taking place at an unusually low temperature in the cooling mode, $T_5 = 46\,\text{K}$, and accompanied by a giant temperature hysteresis in case of heating, $\delta T_5 = 32\,\text{K}$ [8]. Thirdly, another ferroelectric phase can be induced in this crystal either by high hydrostatic pressure, $p > 0.5\,\text{GPa}$ [4,5,8,20], or by deuterization [21]. Fourth, TAHS undergoes a transition from the ferroelastic state to the superionic phase I(R-3m) at 413 K as a result of heating [2,22].

The results of studies using incoherent neutron scattering, as well as neutron and X-ray powder diffraction, allowed concluding that structural distortions during low-temperature phase transitions in TAHS are a caused by changes of the orientation ordering of ammonium ions [12,23]. The data from the study of the effect of even partial substitution of the tetrahedral ammonium cation on spherical rubidium provide a fairly reliable confirmation of this conclusion. For example, ferroelastic phase II is stable up to $\sim 6\,\text{K}$ in crystals $[(NH_4)_{0.82}Rb_{0.18}]_3H(SO_4)_2$ [23] and $[(NH_4)_{0.46}Rb_{0.52}]_3H(SO_4)_2$ (TAHRS) [18], and the orientation disorder of ammonium ions present in the structure of solid solutions turns out to be „frozen“ as a result the transition of the crystal into the dipole glass phase at $T_g \approx 70\,\text{K}$.

Significant changes in TAHS symmetry as a result of the abundance of phase transitions are accompanied by abnormal behavior of thermal expansion and heat capacity [7,24]. Moreover, in the first case, the ratio between the negative and positive linear expansion coefficients due to the anisotropy of a low-symmetric crystal results in significant variations in the values and signs of the volumetric baric coefficients dT/dp. In this regard, studies of barocaloric (BCE) and piezocaloric effects in $(NH_4)_3H(SO_4)_2$ are of undoubted interest, the essence of which lies in the change of the entropy/temperature of a solid body with varying hydrostatic/uniaxial pressures under isothermal/adiabatic conditions. Since it was previously noted that cracking of TAHS crystals is not excluded during phase transitions of the first order, from a practical point of view, it is equally important to obtain information about the implementation of BCE in a ceramic sample. This paper is devoted to solving exactly this kind of problem. Careful studies of the temperature dependences of the heat capacity, thermal expansion and pressure sensitivity of the TAHS ceramic sample were performed, which provided the following outcomes: 1) filling in the missing information about the position of the boundaries between phases III–IV–V on the phase diagram $T-p$ and, thus, obtaining reliable information about the signs and values of the corresponding baric coefficients; 2) performing an analysis of the phase diagram entropy–temperature–pressure and determining the values and dependences on temperature and pressure of extensive and intensive parameters of the barocaloric effect, as well as the integral characteristic — relative cooling capacity.

2. Samples and experimental methods

Colorless single crystals of TAHS were grown by slow evaporation of an aqueous solution of three moles $(NH_4)_2SO_4$ and one mole H_2SO_4 at $\sim 30°C$. Massive crystals with a volume of $1-4\,cm^3$ comprising quasi-hexagonal plates with the most developed face (001) were obtained.

In accordance with the task set in this paper, the first stage included the studies on quasi-ceramic samples in the form of tablets with a diameter of 8 mm and a thickness of 1–2 mm, prepared by pressing (under pressure ~ 1 GPa) of the powder obtained by grinding a single crystal. The ceramics were not heat treated because of the presence of ammonium ions in the structure. The estimated density of ceramics is $\rho \approx 1.823\,g/cm^3$.

X-ray diffraction studies of TAHS ceramic samples were performed at room temperature using Haoyuan powder diffractometer with Cu–K_α radiation and a linear detector. 2θ detector step was $0.01°$ with 0.2 s exposure at each point. The experimental diffractogram and the results of its analysis using the Rietveld method ($R_{wp} = 7.621$, $R_p = 4.964$, $\chi^2 = 4.339$) are presented in Figure 1.

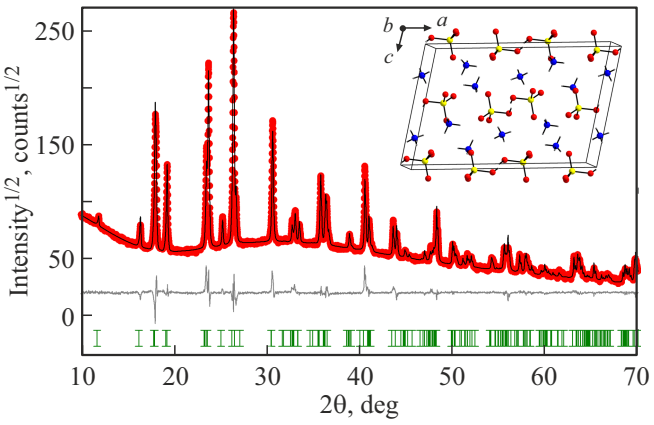

Figure 1. Results of the study of the TAHS structure by the Rietveld method. The insert shows the phase structure $A2/a$.

It was found that, firstly, as expected, the samples are characterized by monoclinic symmetry ($A2/a$, $Z = 4$), secondly, they lack any additional phases and impurities and, thirdly, the parameters of the lattice cell: $a = 15.43719(48)$ Å, $b = 5.86170(21)$ Å, $c = 10.17072(36)$ Å, $\alpha = \gamma = 90$ deg, $\beta = 101.8664(20)$ deg, $V = 900.662(54)$ Å^3 are quite satisfactorily consistent with the previously defined parameters [6,10,15]. The size of crystallites in ceramics varies within the range of 600–1000 nm.

TAHS heat capacity $C_p(T)$ was measured in the temperature range of 80–300 K using an adiabatic calorimeter [25] with an error not exceeding 0.3–0.5%. Discrete ($\Delta T = 0.5-3.0$ K) and continuous ($dT/dt = 0.1-0.3$ K/min) heating modes were used. 0.0635 g sample was mounted on the furniture (heater + screen) using contact lubricant, the heat capacities of which were determined in separate experiments.

The temperature behavior of linear deformation $\Delta L/L_0(T)$ and the coefficient of linear thermal expansion $\alpha(T)$ were measured in the temperature range of 100–350 K using the induction dilatometer NETZSCH DIL-402 C. The measurements were carried out in the heating mode at a rate of 3 K/min in the flow of dry He. The load of the rod on the sample did not exceed 30 cN. A standard made of fused quartz was used to calibrate and account for the expansion of the measuring system. The inaccuracy between the experimental results obtained in several series of measurements did not exceed 2–3%.

According to the results of preliminary calorimetric studies, the entropies of phase transitions in TAHS are either small, or they change in wide temperature ranges [24]. That is, the traditional method of differential thermal analysis for plotting a phase diagram temperature–pressure ($T-p$) appeared ineffective. Therefore, the sensitivity of phase transition temperatures to pressure, $T_i(p)$, was determined by studying the temperature and baric dependences of the capacity of sample $C(T, p)$. The corresponding studies

were performed on a single crystal sample given that phase transitions II−III−IV−V in TAHS have a non-ferroelectric nature and that the dependences $C(T, p)$ in the ceramic sample will certainly be smeared. Silver electrodes made of conductive paste were applied to the largest facets of the plate with dimensions $0.75 \times 6 \times 10$ mm, perpendicular to the axis c. The measurements were carried out in a high-pressure chamber connected via a multiplier to a pumping station. A mixture of silicone oil and pentane was used as a pressure transfer medium. Temperature and pressure were measured with an accuracy of ± 0.3 K and $\pm 10^{-3}$ GPa using a copper−constantane thermocouple and a manganin resistive sensor, respectively.

3. Results and discussion

3.1. Thermal properties

The results of calorimetric studies of TAHS in a wide temperature range are presented in Figure 2, *a* in the form of a temperature dependence of the isobaric molar heat capacity. Abnormal behavior of $C_p(T)$ was detected at three temperatures: $T_2 = 265.8 \pm 0.2$ K; $T_3 \approx 142$ K; $T_4 = 138.9 \pm 0.5$ K, corresponding to phase transitions II−III−IV−V and quite satisfactorily consistent with the data of others studies [7,24].

The dashed line in Figure 2, *a* corresponds to the lattice heat capacity, $C_{\text{lat}}(T)$, determined by approximating the dependences $C_p(T)$ in areas far from the temperatures of structural transformations by a combination of Debye and Einstein functions $C_{\text{lat}}(T) = K_{\text{D}} C_{\text{D}}(T, \Theta_{\text{D}}) + K_{\text{E}} C_{\text{E}}(T, \Theta_{\text{E}})$ (K_{D}, K_{E}, Θ_{D}, Θ_{E} — fitting parameters).

Abnormal heat capacity, $\Delta C_p = C_p - C_{\text{lat}}$, exists in wide temperature ranges, especially at $T < T_2$. The latter circumstance may be associated with the gradual localization of a dynamically disordered acid proton on a hydrogen bond [16].

The presence of ΔC_p in the paraelastic phase, $\sim (T_2 + 35\,\text{K})$, may be attributable not only to a physical cause, but also to a smearing of the heat capacity in the ceramic sample. This assumption is also supported by the barely detectable anomaly $\Delta C_p(T)$ at T_3 (Figure 2, *b*). However, the validity of this assumption can only be verified by direct measurements of single crystal $C_p(T)$, which are planned for the next stage of the study of BCE and PCE in TAHS.

The changes in enthalpy and entropy associated with phase transitions were determined by integrating the corresponding functions $\Delta H_i = \int \Delta C_p dT$ and $\Delta S_i = \int (\Delta C_p/T) dT$: $\Delta H_2 = 2200 \pm 180$ J/mol; $\Delta H_{3+4} = 500 \pm 40$ J/mol; $\Delta S_2 = 8.87 \pm 0.71$ J/(mol · K); $\Delta S_{3+4} = 3.64 \pm 0.29$ J/(mol · K). The information about the integral characteristics for transitions III−IV−V is given in the form of sums because of the weak manifestation of the anomaly at T_3. The temperature dependence of the anomalous entropy in a wide temperature range is shown in Figure 2, *c*. In accordance with the values $\Delta S_2 = 1.07R \approx R \ln 3$ and $\Delta S_{3+4} = 0.44R \ll R \ln 2$, only

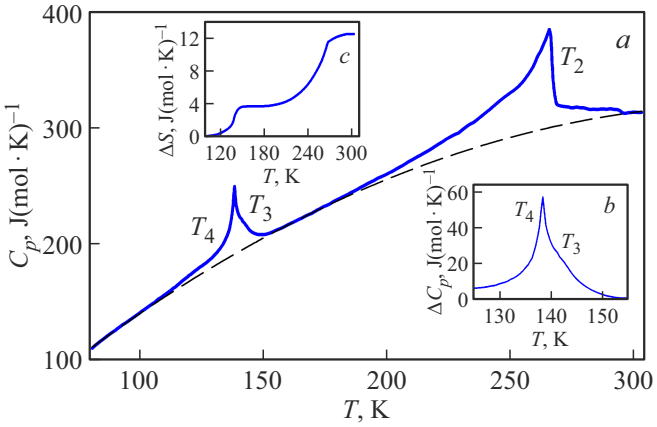

Figure 2. *a* — temperature dependence of the isobaric molar heat capacity of ceramic TAHS. Dashed line — lattice heat capacity. *b* — abnormal heat capacity in the region of phase transitions at T_3 and T_4. *c* — behavior of abnormal entropy in case of successive phase transitions II ↔ III ↔ IV ↔ V.

the transition at T_2 can be confidently considered to be associated with the processes of orientational ordering of ammonium groups, assumed based on the analysis of neutron diffraction study data [23]. As for the structural transformations at T_3 and T_4, the small total entropy parameter is consistent with the conclusions of X-ray diffraction studies on the statistical or dynamic motion in phase II of H atoms involved in hydrogen bonds between shallow double potential minima [6]. That is, in the case of dynamic motion, it is possible to talk about processes in which the lifetimes of an atom H in potential minima are comparable to the hopping times between them. The change in entropy in this case may be greater or less than the values characteristic, respectively, of classical transformations of the displacement type ($\Delta S \approx (0.1-0.2)R$) and the order−disorder ($\Delta S > R \ln 2$), and is determined by the degree of anharmonicity of oscillations of critical atoms, which is characterized by the square of the ratio of the amplitude of ion vibrations to the average interatomic distance [26].

The change of the linear size along the diameter of a cylindrical sample was determined in dilatometric experiments. It was impossible to perform X-ray study to determine the presence/absence of texture in ceramic samples TAHS because of the small area of the tablet's generatrix. Therefore, we considered it possible to use the following generally accepted relationships between volumetric and linear, experimentally measured, thermal expansion characteristics $\Delta V/V_0(T) = 3(\Delta L/L_0)(T)$ and $\beta(T) = 3\alpha(T)$. The temperature dependences of the volumetric deformation and the coefficient of volumetric thermal expansion are shown in Figure 3.

As in the case of heat capacity, anomalies of thermal expansion associated with phase transitions are most pronounced in the form of sharp peaks at temperatures of $T_2 = 266.8 \pm 1.0$ K and $T_4 = 142 \pm 1$ K, and the transi-

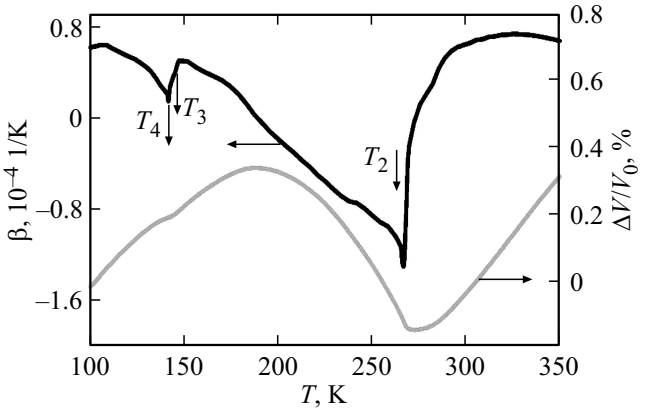

Figure 3. Temperature dependences of volumetric deformation $\Delta V/V_0(T)$ and the coefficient of volumetric thermal expansion $\beta(T)$.

tion III−IV is characterized only by a small projection on the dependence $\beta(T)$ at $T_3 \approx 145$ K. Some difference in the values of T_i determined in calorimetric and dilatometric experiments is attributable to the fact that the measurements of $C_p(T)$ and $(\Delta L/L_0)(T)$ were performed under different thermodynamic conditions. The conditions for measuring the heat capacity in an adiabatic process at a heating rate significantly lower than the rate in thermal expansion measurements are closer to equilibrium.

A remarkable feature of ceramic TAHS is the presence of a negative coefficient of volumetric thermal expansion in a wide temperature range of $\sim (190-270)$ K (Figure 3), which, as will be shown below, is the reason for the implementation of reverse BCE in ceramic TAHS. The presence of an abnormal contribution $\Delta\beta(T)$ significantly above T_2 is consistent with the presence and behavior of abnormal heat capacity in paraelastic phase II.

3.2. Phase $T-p$-diagram

The capacity $C(T, p)$ of a TAHS-based capacitor in case of heating were was studied in the pressure range of 0−0.3 GPa. The behavior of $C(T)$ at $p = 0$ is consistent with the temperature dependence of the dielectric constant studied earlier in the same temperature range [3]. Anomalies of $C(T)$ associated with phase transitions in the studied sample were observed at temperatures close to those established in calorimetric and dilatometric experiments: $T_2 = 265.4 \pm 1.0$ K; $T_3 = 141.5 \pm 1.5$ K; $T_4 = 138.0 \pm 1.0$ K. The position of T_3 and T_4 corresponds to two characteristic points of change of behavior of $C(T)$, associated respectively with the beginning of a stepwise decrease of capacity and with the maximum derivative dC/dT (Figure 4, *b*). The temperature T_2 was determined, as in Ref. [3], by a break in the temperature dependence of the reverse capacity $1/C$ (Figure 4, *c*).

Two more pronounced anomalies were found on the curve $C(T)$ at temperatures ~ 220 and ~ 250 K (Figure 4, *a*), which were also previously observed and proposed hypothetical reasons for their appearance [3,27]. In the first case, it was believed that the dielectric relaxation characteristic of glass-like materials and observed at $T > 220$ K, is the result of the reorientation of dipole molecular groups H_2SO_4 or HSO_4^- obtained by random localization of acidic protons in statically disordered hydrogen bonds O−H · · · O [27]. The nature of the diffuse peak in the region of 250 K was explained based on the analysis of the two-lattice model of the TAHS structure by a gradual change in the polarization of the sublattices, which at a pressure above 0.5 GPa results in the occurrence of two ferroelectric phases [4].

Previously, in experiments with hydrostatic pressure, the authors of Ref. [4,5,8,20], without explaining the reasons, limited themselves only to studying the temperature region where the phase transition II−III occurs. And the part of the phase $T-p$-diagram associated with transitions III−IV−V was reconstructed from data of baric coefficients dT_3/dp and dT_4/dp calculated from the Clapeyron−Clausius and Ehrenfest ratios using data obtained with $p = 0$ [7].

It is clear from the dependences $C(T, p)$ defined in this paper that anomalies, both related and unrelated to phase transitions, are slightly influenced by pressure, at least in the studied range of p (Figure 4).

A part of the $T-p$ phase diagram in the pressure range of 0−0.3 GPa was plotted as a result of studies performed in heating and pressure increase modes, on which, in particular, the results of direct experimental measurements of the dependences $T_3(p)$ and $T_4(p)$ were shown for the first time (Figure 5). The values of the baric coefficients $dT_2/dp = -49.4 \pm 2.5$ K/GPa, $dT_3/dp = -21.8 \pm 2.5$ K/GPa and $dT_4/dp = -30.8 \pm 1.5$ K/GPa are in satisfactory agreement with the data obtained earlier for transition II−III by direct measurements [5] and for transition IV−V by calculations [7].

However, although the experimental results with respect to dT_3/dp and dT_4/dp indicate an expansion of the temperature stability region of phase IV under pressure, the temperature T_3 decreases at the same time, which is inconsistent with its increase, following from calculations within the Ehrenfest equation [7]. The reason for the different signs dT_3/dp, in our opinion, is most likely related to the difficulties of reliable determination of the jumps of the coefficient of linear thermal expansion $\Delta\alpha_i$ in case of the transition of the second order and, as a result, the value $\Delta\beta = \Sigma\Delta\alpha_i$ used in the calculations of the baric coefficient [7]. The negative sign of anomalies $(\Delta V/V)(T)$ and $\beta(T)$ for ceramic TAHS at temperatures T_2, T_3 and T_4 (Figure 3) corresponds to their decrease under pressure which was experimentally established (Figure 5).

Both diffuse anomalies found on the curve $C(T)$ in phase III become more pronounced with the increase of pressure (Figure 4, *a*) and the dependence of temperatures of their maxima on pressure is close to the value dT_2/dp (Figure 5).

3.3. Barocaloric effect

The physical interpretation of the barocaloric effect is based on the consideration of the differential equation $(\partial S/\partial p)_T = -(\partial V/\partial T)_p$, which follows from the expression for the Gibbs energy: $d\Phi = -SdT + Vdp$. Reversible changes of entropy in the isothermal process (extensive BCE) are accepted as the main criteria for the barocaloric efficiency of materials

$$\Delta S_{\mathrm{BCE}}(T, p) = S(T, p) - S(T, 0) \tag{1}$$

and temperatures in the adiabatic process (intensive BCE)

$$\Delta T_{\mathrm{AD}}(T, p) = T(S, p) - T(S, 0) \tag{2}$$

as a result of changes of the external hydrostatic pressure $0 \leftrightarrow p$.

Obviously, BCE, being associated with thermal expansion, is characteristic of any physical systems. However, abnormally large caloric effects associated with a significant increase of the value of the derivative $(\partial V/\partial T)_p$ with changes of the symmetry of the crystal lattice can be observed in solids undergoing phase transitions, in addition to the trivial BCE caused by thermal expansion of the crystal lattice. And, of course, it should be borne in mind that both barocaloric characteristics, ΔS_{BCE} and ΔT_{AD}, largely depend on the sensitivity of materials to pressure changes, that is, on the value of the baric coefficient dT/dp, characterizing the displacement of the transition temperature under pressure. Since in the near future we plan to conduct comparative studies of the features of the development of phase transitions and the occurrence of BCE related to the size factor of TAHS samples (single crystal and ceramic polycrystal), we limit ourselves in this paper to determining the parameters of BCE only in case of structural transformations in ceramics.

In accordance with (1) and (2), extensive and intensive barocaloric parameters can be determined by analyzing the diagram $S-T-p$, where S is the total entropy of the system, which is the sum of the lattice and anomalous contributions determined by integrating the corresponding components the heat capacities presented above (Section 3.1)

$$S(T) = S_{\mathrm{lat}}(T) + \Delta S(T) = \int (C_{\mathrm{lat}}/T)dT + \int (\Delta C_p/T)dT. \tag{3}$$

However, it is more convenient to consider the two-coordinate diagram entropy–temperature, which shows the dependences $S(T)$ corresponding to different pressures. In this case, the position of the abnormal entropy at these pressures $\Delta S(T, p)$ is determined by the shift of the function $\Delta S(T, 0)$ at $p = 0$ along the temperature scale in accordance with the baric coefficient dT/dp

$$\Delta S(T, p) = \Delta S(T + p\,dT/dp, 0). \tag{4}$$

It was assumed that the entropies of phase transitions II–III, III–IV and IV–V, as well as the degree of their proximity to the tricritical point, do not depend on pressure. Since it was not possible to distinguish the abnormal contributions to entropy at T_3 and T_4 in calorimetric experiments on a ceramic sample, and the values of dT_3/dp

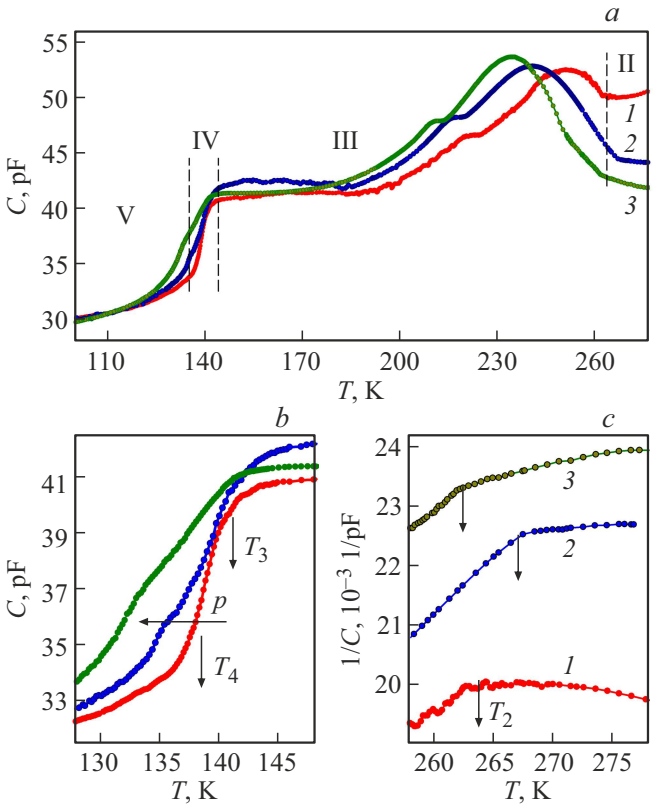

Figure 4. Temperature dependences of the capacity, $C(T)$, along the axis c of the TAHS crystal at pressures, GPa: *1* — 0, *2* — 0.10, *3* — 0.17 in a wide temperature range (a) and in the vicinity of T_3 and T_4 (b), as well as the reverse capacity, $1/C$, in regions of transition II–III (c). Vertical dashed lines — phase boundaries at $p = 0$.

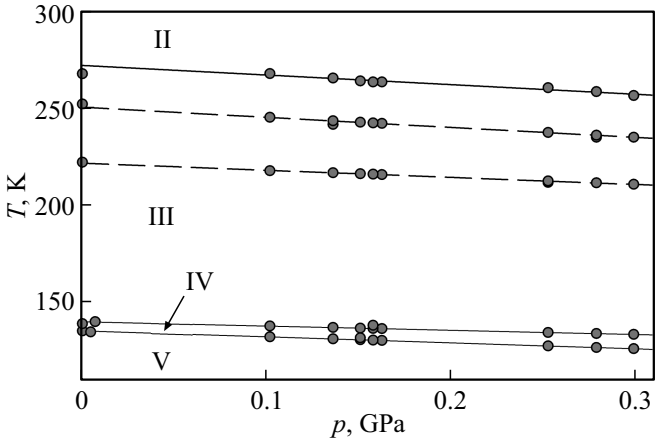

Figure 5. Phase $T-p$-diagram. The dashed lines correspond to changes in the temperature of anomalies in the region of 220 and 250 K (at $p = 0$), which are not associated with phase transformations.

Absolute and integral barocaloric parameters in a number of related sulfates at $p = 0.5$ GPa. * — data of this study

Material	ΔS_{BCE}, J/kg · K	ΔT_{AD}, K	RCP, J/kg	δT, K	dT/dp, K/GPa	p_{rev}, GPa	Literature
$(NH_4)_2SO_4$	100.0	−13.3	2600	1.0	−49	0.02	[29]
NH_4HSO_4	65.5	−11.0	3500	2.5	−123	0.02	[30,31]
$(NH_4)_3H(SO_4)_2$	19.4	−3.7	800	0	−49	0	*

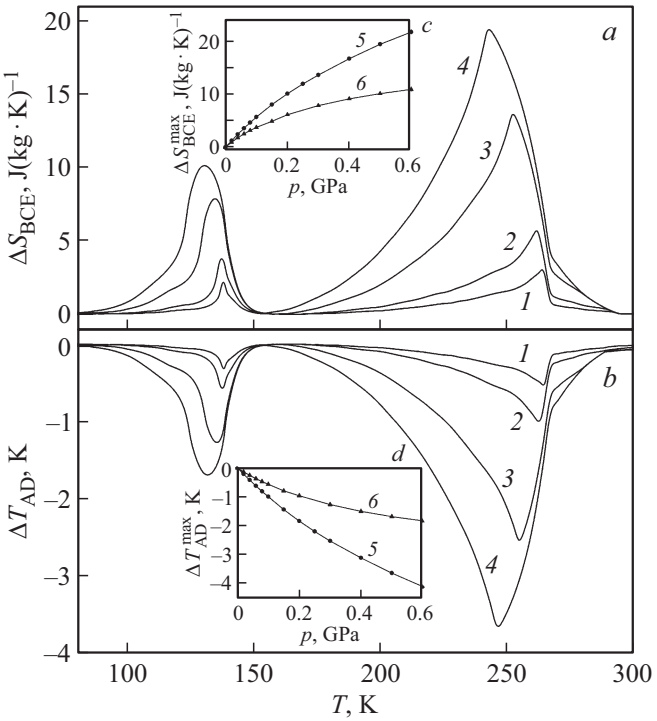

Figure 6. Temperature dependences of extensive ΔS_{BCE} (a) and intensive ΔT_{AD} (b) BCE in the region of phase transitions II−III−IV−V at pressures, GPa: *1* — 0.05; *2* — 0.10; *3* — 0.30; *4* — 0.50. Dependences of the maximum values of extensive (c) and intensive (d) BCE on pressure at T_2 (*5*) and $T_3 + T_4$ (*6*).

and dT_4/dp are quite close, the dependences of $S(T, p)$ in the field of phase transitions III−IV−V are practically inseparable and look like a common function.

The barocaloric effects in TAHS are reversed in accordance with the negative signs of the baric coefficients of the structural transformations studied by us, that is, an increase of hydrostatic pressure results in an increase of entropy and a decrease of temperature. Figures 6, a and 6, b show the behavior of extensive and intensive BCE associated with a sequence of structural transitions II−III−IV−V.

If the thermal expansion of the crystal lattice is excluded from the analysis of the contribution to the BCE, the maximum values of the extensive and intensive parameters are limited by the value of the entropy of the phase transition [28]. For TAHS, these values are equal to: $(\Delta S^{max}_{BCE})_{T2} = \Delta S_2 = 35.9$ J/kg · K, $(\Delta T^{max}_{AD})_{T2} = -7.8$ K; $(\Delta S^{max}_{BCE})_{T3+T4} = \Delta S_{3+4} = 14.7$ J/kg · K, $(\Delta T^{max}_{AD})_{T3+T4} = 2.9$ K. Figures 6, c and 6, d demonstrate the nature of changes of barocaloric parameters, ΔS^{max}_{BCE} and ΔT^{max}_{AD}, in case of increase of pressure. BCE requires quite large and at the same time different pressures for achieving the maximum possible values of both parameters, since ΔT_{AD} also depends to a greater extent on the derivative dS/dT: $(\Delta S^{max}_{BCE})_{T2} - p \approx 2.2$ GPa, $(\Delta T^{max}_{AD})_{T2} - p > 3.0$ GPa; $(\Delta S^{max}_{BCE})_{T3+T4} - p = 1.7$ GPa, $(\Delta T^{max}_{AD})_{T3+T4} - p > 2.5$ GPa.

It was said above that the absolute values of extensive and intensive BCE are usually considered as one of the main criteria for evaluating the prospects of using the material as a solid-state refrigerant. TAHS is inferior to other ferroid materials in both parameters related to the structural transformation at T_2. From our point of view, a comparison with BCE in related sulfates $(NH_4)_2SO_4$ [29] and NH_4HSO_4 [30,31] presented in the table is the most informative in this regard.

However, TAHS is characterized by a number of other equally important advantages. Firstly, due to the presence of the anomalous entropy of the transition II−III in a very wide temperature range of $\sim$ (150−290) K and as a result ΔS_{BCE}, a very important integral barocaloric parameter — relative cooling power (RCP) is worth attention [32]) (see table)

$$\mathrm{RCP} = \Delta S^{max}_{BCE} \cdot \Delta T_{FWHM}, \qquad (5)$$

here ΔT_{FWHM} — full width at half maximum $(\Delta S_{BCE})_p$.

Secondly, phase transition II−III is a transformation of the second order. The related absence of temperature hysteresis, $\delta T = 0$, guarantees a very high reversibility of BCE compared to $(NH_4)_2SO_4$ and NH_4HSO_4, experiencing transitions of the first order, $\delta T > 0$ (see table). That is, the paths of the components of the forward and reverse processes coincide in case of thermo- and barocycling within the thermodynamic cooling cycle based on TAHS as a refrigerant, which allows avoiding significant heat losses. The pressure required to achieve a reversible BCE in the case of a transition of the first order can be estimated using the expression, $p_{rev} = \delta T/|dT/dp|$ [33]. Although for $(NH_4)_2SO_4$ and NH_4HSO_4 this pressure turned out to be quite low (see table), it should be borne in mind that baric hysteresis is also inevitable and of course it will also make a certain contribution to heat losses during the thermodynamic cycle.

Very interesting, from our point of view, is the experimentally established fact that the phase transitions in the sulfates presented in the table, as, by the way, in acidic selenate NH_4HSeO_4 [34], are characterized by negative

the values of the baric coefficients, $dT/dp < 0$, which is the reason for the occurrence of the reverse BCE in them. Since the coefficient of volumetric thermal expansion away from structural transformations in these materials is usually positive, taking this phenomenon into account in the analysis within the framework of $(1)-(4)$ results in a decrease of the total parameters of the BCE [29,30]. However, sulfates/selenates are characterized by a significant anisotropy of linear thermal expansion due to the rather low symmetry, which does not exclude the existence of crystallographic directions in them in which the signs of contributions to the PCE associated with the abnormal behavior of $\Delta\alpha(T)$ in case of phase transitions and linear expansion of the crystal lattice $\alpha_{\text{lat}}(T)$ coincide.

4. Conclusion

The heat capacity, thermal expansion and sensitivity to hydrostatic pressure of ceramic triammonium hydrodisulfate $(NH_4)_3H(SO_4)_2$ (TAHS) was experimentally studied. The main thermodynamic parameters of successive phase transitions $II \leftrightarrow III \leftrightarrow IV \leftrightarrow V$ were determined: abnormal changes of entropy and deformations, as well as baric coefficients, which allowed, in particular, eliminating the „white spot“ on the phase diagram temperature–pressure associated with the position of the boundaries of phases III, IV and V. The presence of a negative coefficient of volumetric expansion was found in a wide temperature range $(190-270)$ K of phase III, which determines the occurrence of the reverse BCE in TAHS.

The phase diagram entropy–temperature–pressure was analyzed and the temperature and baric dependences of the BCE parameters were determined. In terms of absolute barocaloric values, TAHS is inferior to other ferroid materials, in particular, related sulfates/selenates. However, its obvious advantages include the following. Firstly, the second order of phase transition II–III, characterized by the highest BCE parameters, guarantees almost complete reproducibility of the thermo- and barocycling processes. Secondly, the presence of the corresponding barocaloric entropy in a very wide temperature range of phases II and III suggests a significant value of the relative cooling capacity even at low pressures and the possibility of organizing a thermodynamic refrigeration cycle in the same temperature range.

Acknowledgments

Radiographical and dilatometric data were obtained using the equipment of the Krasnoyarsk Regional Center for Collective Use of the Federal Research Center „Krasnoyarsk Scientific Center of the Siberian Branch of the Russian Academy of Sciences“.

Funding

The study was supported by the grant of the Russian Science Foundation No. 23-22-10014, Krasnoyarsk Regional Science Foundation, https://rscf.ru/en/project/23-22-10014/.

Conflict of interest

The authors declare that they have no conflict of interest.

References

[1] P. Palache, H. Berman, C. Frondel. Dana's System of Mineralogy, Vol. II: Halides, Nitrates, Borates, Carbonates, Sulfates, Phosphates, Arsenates, Tungstates, Molybdates, Etc. (Seventh Edition). John Wiley and Sons, Inc., N.Y. (1960).
[2] B. Gossner. Z. Kristallogr. **38**, 110 (1904).
[3] K. Gesi. Phys. Status Solidi A **33**, 479 (1976).
[4] K. Gesi. J. Phys. Soc. Japan **41**, 1437 (1976).
[5] K. Gesi, K. Ozawa. J. Phys. Soc. Japan **43**, 570 (1977).
[6] Sh. Suzuki, Ya. Makita. Acta Cryst. B **34**, 732 (1978).
[7] Sh. Suzuki. J. Phys. Soc. Japan **47**, 1205 (1979).
[8] K. Gezi. Jpn. J. Appl. Phys. **19**, 1051 (1980).
[9] M. Fujimoto, B.V. Sinha. Ferroelectrics **46**, 227 (1983).
[10] A. Leclaire, M. Ledesert, J.C. Monier. Acta Cryst. B **41**, 209 (1985).
[11] M. Kamoun, M.H. Ben Ghozlen, A. Daoud. Phase Transit. **9**, 247 (1987).
[12] R.H. Chen, L.-M. Wang, S.C. Yang. Phase Transit. **37**, 141 (1992).
[13] V.V. Sinitsyn, A.I. Baranov, E.G. Ponyatovsky. FTT **37**, 2059 (1995). (in Russian).
[14] R.H. Chen, T.M. Chen, C.S. Shern. J. Phys. Chem. Solids **61**, 1399 (2000).
[15] K. Friese, I. Aroyo, L. Schwalowsky, G. Adiwidjaja, U. Bismayer. J. Solid State Chem. **165**, 136 (2002).
[16] P.M. Dominiak, J. Herold, W. Kolodziejski, K. Woźniak. Inorg. Chem. **42**, 1590 (2003).
[17] R. Sobiestianskas, J. Banys, A. Brilingas, J. Grigas, A. Pawłowski, B. Hilczer. Ferroelectrics **348**, 75 (2007).
[18] K.-S. Lee, J.-H. Ko. J. Korean Phys. Soc. **74**, 695 (2019).
[19] G.J. McIntyrea, L.S. Smirnov, A.I. Baranov, V.V. Dolbinina, M.V. Frontasyeva, S.S. Pavlov, Yu.S. Pankratova. Crystallogr. Rep. **58**, 78 (2013).
[20] K. Gesi. J. Phys. Soc. Japan **41**, 1941 (1977).
[21] T. Osaka, Y. Makita, K. Gesi. J. Phys. Soc. Japan **43**, 933 (1977).
[22] V.V. Sinitsyn, A.I. Baranov, E.G. Ponyatovsky, L.A. Shuvalov. Solid State Ion. **77**, 118 (1995).
[23] L.S. Smirnov, A.I. Baranov, L.A. Shuvalov, L. Bobrovich-Sarga, I. Natkanets, S. Vala. FTT **43**, 115 (2001). (in Russian).
[24] Sh. Suzuki, Ya. Oshino, K. Gesi, Ya. Makita. J. Phys. Soc. Japan **47**, 874 (1979).
[25] A.V. Kartashev, I.N. Flerov, N.V. Volkov, K.A. Sablina. FTT **50**, 2027 (2008). (in Russian).
[26] V.G. Vaks. Vvedenie v mikroskopicheskuyu teoriyu segnetoelektrikov. Nauka, M. (1973). 327 s. (in Russian).
[27] H.K. Shin. Solid State Commun. **128**, 131 (2003).
[28] R. Pirc, Z. Kutnjak, R. Blinc, Q.M. Zhang. Appl. Phys. Lett. **98**, 021909 (2011).

[29] E.A. Mikhaleva, I.N. Flerov, M.V. Gorev, V.S. Bondarev, E.V. Bogdanov. Crystals **10**, 51 (2020).
[30] M.V. Gorev, E.A. Mikhaleva, I.N. Flerov, E.V. Bogdanov. J. Alloys Compd. **806**, 1047 (2019).
[31] E.A. Mikhaleva, M.V. Gorev, M.S. Molokeev, A.V. Kartashev, I.N. Flerov. J. Alloys Compd. **839**, 155085 (2020).
[32] A.M. Tishin, Y.I. Spichkin. The Magnetocaloric Effect and its Applications. Institute of Physics Publishing, Bristol (2003). 475 p.
[33] A. Aznar, P. Lloveras, M. Barrio, P. Negrier, A. Planes, L. Mañosa, N.D. Mathur, X. Moya, J. Tamarit. J. Mater. Chem. A **8**, 639 (2020).
[34] V.S. Bondarev, E.A. Mikhaleva, M.V. Gorev, M.S. Molokeev, I.N. Flerov, E.V. Bogdanov, A.V. Cherepakhin. Solid State Sci. **148**, 107440 (2024).

Translated by A.Akhtyamov